Bioorganic & Medicinal Chemistry 26 (2018) 266–277

Contents lists available at ScienceDirect

Bioorganic & Medicinal Chemistry

journal homepage: www.elsevier.com/locate/bmc

Design, synthesis and biological evaluation of novel indole-xanthendione hybrids as selective estrogen receptor modulators

Ramit Singla [a], Kunj Bihari Gupta [b], Shishir Upadhyay [c], Monisha Dhiman [b], Vikas Jaitak [a,*]

[a] Centre for Pharmaceutical Sciences and Natural Products, Central University of Punjab, Bathinda, India
[b] Centre for Biochemistry and Microbial Sciences, Central University of Punjab, Bathinda, India
[c] Centre for Animal Sciences, Central University of Punjab, Bathinda, India

ARTICLE INFO

Article history:
Received 1 September 2017
Revised 27 October 2017
Accepted 25 November 2017
Available online 1 December 2017

Keywords:
Breast cancer
Estrogen receptor alpha
Indole-xanthendione hybrids
RT-PCR SERM
Western blotting

ABSTRACT

Ground breaking clinical therapeutic advances in the treatment of breast cancer (BC) is the introduction of selective estrogen receptor modulators (SERMs). We have expeditiously designed and synthesized indole-xanthendione hybrids by coalescing the indole nucleus with xanthendione. All the compounds were first screened for anti-proliferative activity, cytotoxicity and ER-α binding affinity by utilizing ER-α dominant T47D BC cell lines, PBMCs and ER-α competitor assay kit. From this study, two representative compounds **6e** and **6f** showing most promising activity were advanced for gene expression studies for targeting ER-α. Cell imaging experiment undoubtedly indicate that both the compounds were able to cross cellular bio membrane and accumulate thus instigating cytotoxicity. RT-PCR and Western blotting experiments further strengthened that both compounds altered the expression of mRNA and receptor protein of ER-α, thereby forestalling downstream transactivation and signalling pathway in T47D cells line. Structural investigation from induced fit simulation study suggest that indole moiety of the compounds **6e** and **6f** helps in the anchoring of the xanthendione moiety in the hydrophobic region of the cavity thus enabling the compound to bind in antagonistic conformation similar to bazedoxifene by extensive hydrogen bonding and Van der Waals forces. All these finding collectively imply that compound **6e** and **6f** represents a novel potent ER-α antagonist and in the development of SERMs for the management of BC.

© 2017 Elsevier Ltd. All rights reserved.

1. Introduction

Selective Estrogen Receptor Modulators (SERMs) are chemical entities that alter the action of estrogen by binding to estrogen receptors (ERα or ERβ subtypes) in cells. ERs are activated by estradiol produced by the ovaries. Once estradiol binds to the ER, the conformation of the ER gets changed and coactivator binds to it. The ER-coactivator complex binds to the promoter region of genes and downstream transcriptional pathways are sequentially activated. Thus, the proliferation of breast cancer cells is promoted by estradiol. Inhibition of ER activation is thus important for the development of drugs targeting breast cancer (BC).[1,2] Since the first clinical use of tamoxifen as a SERM in 1971, second and third generation SERMs have been developed for combating the ER responsive BC and to avoid the uterotrophic effects of tamoxifen. These include raloxifene, lasofoxifene and more recent the indole containing compounds bazedoxifene.[3,4]

During the recent development in SERMs, two drug candidates were moved to clinical evaluations, which were 2-phenylindole analogs, bazedoxifene[5] and pipendoxifene. Bazedoxifene is approved in the European Union and under review by US FDA for the prevention and treatment of postmenopausal osteoporosis. Upon approval, it will be solely marketed by Pfizer under the trade-name Viviant in the US and Conbriza in the EU. Bazedoxifene binds to ER-α with higher affinity as compared to ER-β.[6] It has been reported that the inhibitory effect of bazedoxifene is associated with ER-α down-regulation and cell cycle arrest.[7] In recent times, combination of bazedoxifene with palbociclib have been used for treatment of metastatic BC at stage IV.[8,9]

The most promising attributes of hybrid molecules of mixed biosynthetic origin led to the idea of generating novel small heterocyclic molecular entities by rationally combining two or more different classes of compounds of natural or synthetic origin. The expected outcome being that combination of structural features of two or more functionally active substances into one molecule may lead to synergism, enhancement or modulation of the desired characteristics of individual components. Another tempting

* Corresponding author.
E-mail addresses: vikasjaitak@gmail.com, vikas.jaitak@cup.edu.in (V. Jaitak).

https://doi.org/10.1016/j.bmc.2017.11.040
0968-0896/© 2017 Elsevier Ltd. All rights reserved.

feature of this approach is that it opens the ventures of myriad possibilities for generating a diverse array of pharmacophore which have an immense application in the field of medicinal chemistry. The molecular hybrids can also address the problem of incidence of drug resistance to cancer chemotherapeutic agents because a single molecule containing more than one pharmacophore, each with different mode of action, could be beneficial for the treatment of cancer and can reduce the chances of drug resistance.[10–12]

Many of the current chemotherapy drugs have low specificity for tumour cancer cells, and are also toxic to normal cells. Indeed, one of the biggest challenges of combating cancer is the development of new anticancer agents that are safe and effective. It has been reported that 2-arylindole derivative are selective towards the ER-α and antagonize the action of oestradiol in BC cells and uterus tissues[2]. Xanthenones are important biologically active heterocyclic compounds, with remarkable biological and medicinal properties.[13–15] Taking these structural features in account, in the present study we have designed and synthesised novel indole-xanthendione derivatives as putative SERM for targeting ER-α for the management of hormone dependent BC (HDBC). The synthesised molecules were characterised by NMR, IR and HRMS. Compounds were analysed for the anticancer activity using ER-α expressing T47D cell lines, ER-α binding assay, RT-PCR, western blotting and confocal microscopy. Molecular docking was used to identify, the possible binding modes of indole- xanthendione derivatives with ER-α.

2. Results and discussion

2.1. Design and synthesis Indole-xanthendione derivatives

Xanthones and xanthediones derivatives isolated from natural resources as well as chemically synthesised have been known to inhibit BC proliferation which have been evaluated using BC cell lines.[14,16–21] QSAR analysis of synthesised xanthenone compounds suggests that incorporation and increasing the accessible surface area of hydrogen bond donor atoms at the receptor site leads to an increase in biological activity of the compound.[22] Compounds 12-(4-hydroxyphenyl)-9,9-dimethyl-7a,8,9,10,11a,12-hexahydro-11*H*-benzo[*a*]xanthen-11-one (6.7 μg/mL) were most potent in MCF-7, and showed more activity than the anti-BC drug tamoxifen (10 μg/mL).[23] Phenyl substituted dioxooctahydroxanthenes derivatives have been found to be active in MCF-7 cell lines with an IC_{50} value of 0.02μMol/l.[13]

Structural analysis from the available literature suggests that 1-benzyl-indole-3-carbinol, which is an analog of indole-3-carbinol (I3C) was found to be thousand times more potent in comparison to indole-3-carbinol in suppression of both estrogen dependent and independent BC cell lines.[2,24,25] 2-arylindole derivative have shown one hundred thirty times fold selectivity towards the ER-α (human ER-α/β IC_{50} 2/259 nM) and antagonize the action of estradiol in MCF-7 (IC_{50} 30 nM) cancer cells and uterus tissues.[26] ERA923 is an indole derivative anti-estrogenic compound, equally effective as tamoxifen and overcome the resistance associated with tamoxifen, tested *in vitro* and *in vivo*.[27] For a molecule to act as xenoestrogen/phytoestrogen it must possess certain indispensable characteristics (Fig. 1).

The pharmacophore must contain hydroxyl which mimics the 3-OH and 17β-OH of estradiol. The distance between the 3-OH and 17β-OH must be similar. The pharmacophore must have hydrophobic characteristics and ring structural backbone. It has been observed that nucleic acid bases can exist in multiple tautomeric forms due to the presence of solvent-exchangeable protons which catalyse acid–base autolytic cleavage reactions of self-cleaving ribozymes, such as hairpin, hammerhead, and *glmS*.[28] Similarly, there are chances of formation of enolates as observed in case of atorvastatin and repaglinide which is actively gets converted into its enolate form when dissolved in water and acts on the target site.[29,30] In view of these observations xanthendiones

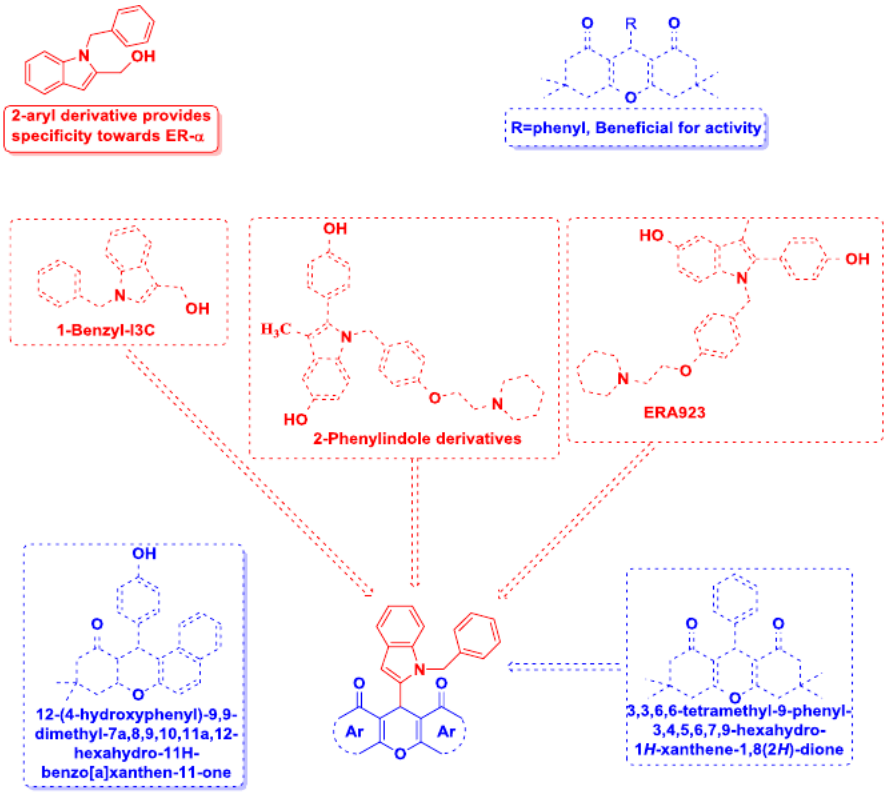

Fig. 1. Designing strategy of indole-xanthendione hybrids.

derivatives designed can exist in keto-enol tautomerism in biological environment thereby giving rise to the hydroxyl groups which mimics the estradiol and the distance between the O—O of hydroxyl group is also similar. The 2-benzyl indole back bone is hydrophobic in nature. Thereby, combining the structural features of the known active compounds and receptor topography the designed compounds are expected to be beneficial in BC management by targeting its proliferation pathways. As these molecules will tend to bind to the estrogenic receptor with greater binding affinity and act as a competitive inhibitor but will not be able to activate the receptor, thereby preventing the downstream transcriptional pathways.

The indole-xanthendione hybrids (**6a-m**) were synthesised by the general route with high to moderate yields as described in Scheme 1. The *N*-position of the starting material ethyl indole-2-carboxylate (**1**) was benzylated using benzyl bromide in the presence of potassium hydroxide using DMSO as polar aprotic solvent to give ethyl-1-benzyl-1H-indole-2-carboxylate (**2**). Compound **2** was reduced to (1-benzyl-1H-indol-2-yl) methanol (**3**) in presence of $LiAlH_4$ under dry THF conditions. Compound **3** was oxidised to 1-benzyl-1H-indole-2-carbaldehyde (**4**) by using activated manganese dioxide in dry CH_2Cl_2. Microwave irradiated aqueous condition in the presence PEG 6000, accelerates knoevenagel condensation and subsequent michael addition of appropriate dimedone with aldehyde (**4**) to form **5**. The compound **5** was cyclized using dry CH_2Cl_2 in the presence of DCC, to afford indole-xanthendione hybrids (**6a-m**) via elimination of water molecule. It should be noted that compounds **6a-m** hitherto unknown in chemical literature and were purified using flash chromatography and unambiguously characterised spectroscopically using ^1H, ^{13}C-NMR and HRMS.

2.2. Biological evaluation of Indole-xanthendione derivatives

SERMs have been developed for targeting and management of HDBC. HDBC is primarily known to proliferate due to the imbalance in the expression of ER-α and ER-β. We have selected T47D cells line for the biological evaluation of the synthesised compounds as these cell line shows dominant expression of ER-α (9/1 ratio of ER-α/ER-β expression).[31,32] All the fourteen synthesised indole-xanthendione derivatives (**6a-m**) were evaluated for the antiproliferative activity using MTT assay at 1, 5, 25 μM concentration and bazedoxifene was taken as standard drug. The anti-proliferative activity of four compounds (**6b**, **6c**, **6e**, **6f**) was comparable to bazedoxifene (16.43 ± 0.94 μM), while other derivatives **6a**, **6d**, **6g**, **6k** and **6l** have shown moderate antiproliferative activity (Table 1, Fig. 2). Compounds were exhibiting dose dependent increase in anti-proliferative activity. Compound **6e** and **6f** were unveiling most promising anti-proliferative activity with IC_{50} value of 16.51 ± 0.75 and 17.94 ± 1.0 μM. Upon analysing the overall structural features and anti-proliferative activity of synthesised derivatives, it was evident that, substitution of the xanthendione moiety with bulkier group decreases the antiproliferative activity (**6g**, **6h**, **6i**, **6j**, **6i** and **6m**).

Further, in order to determine the cytotoxicity of the compounds on the normal cell lines, screening was carried out on human PBMCs (Peripheral Blood Mononuclear Cells) using MTT assay. The results obtained indicated that all the compounds were not showing cytotoxicity even at higher concentration of 100 μM (data not shown). The essential requirement for a SERM compound is to have strong and competitive ER-α binding affinity, and to prevent the trigger of downstream signalling. In view of this, all the synthesised compounds were screened for determining their binding affinity towards ER-α. ER-α competitor assay kit (Polar Screen ER-α Competitor Assay Kit, Green, Life Technology) was utilised for determining the binding affinity. The assay works of the principle that if the compound under analysis does not have binding affinity for the ER-α, then it will not be able to displace the fluorochrome tagged oestradiol (Fluormone™ ES2) from the ER-α-Fluormone™ ES2 complex, thereby give rise to high florescence. On the contrary, low florescence is observed if the compound competitively binds to ER-α by displacing the fluorochrome tagged oestradiol. This change in the florescence provides the relative affinity of the compound under analysis for ER-α. Bazedoxifene was also included as standard in the study.

From the competitive binding assay, it was found that compounds **6c**, **6d** and **6f** were able to bind more efficiently and with higher binding affinity in comparison to the bazedoxifene (31.71 ± 1.41 nM) (Table 1). Whereas, compounds **6e**, **6g**, **6k** and **6l** were having the activity in the range of 51.19–61.08 nM which is slightly higher, as compared to the binding affinity of bazedoxifene at receptor level. While other derivatives **6a**, **6b**, **6g**, **6j** and **6l** were showing moderative activity (Table 1). Compounds **6h**, **6i** and **6m** failed to show significant activity at concentration up to 1000 nM and hence were considered inactive. Upon analysing the of ER-α binding assay and structural features of the derivatives, it was found that presence of at least one unsubstituted cyclohexanone constituting the xanthedione moiety as in compounds **6d**, **6e** and **6f** improves the binding affinity of the compound towards the ER- α receptor.

Paralleling the outcomes of anti-proliferative assay with ER-α binding assay, it was observed that compounds (**6a** and **6b**) were showing impressive anti-proliferative activity but a weak ER-α binding affinity. These compounds may be acting via alternate

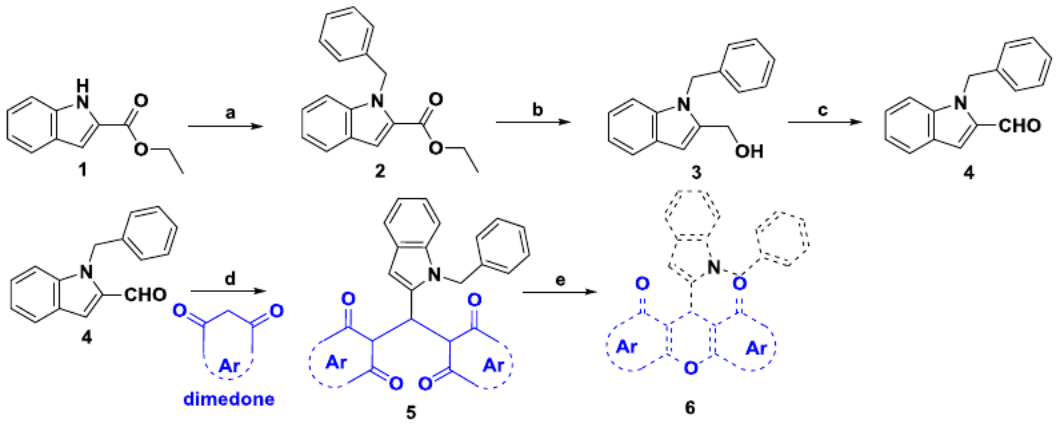

Scheme 1. Reagent and conditions (a) Benzyl bromide, KOH, DMSO, 1.5 h (b) $LiAlH_4$, dry THF, 0 °C, 30 min (c) activated MnO_2, dry CH_2Cl_2, r.t., 5 h (d) corresponding dimedone, PEG 6000, water, MW., 2.5 h (e) DCC, r.t., dry CH_2Cl_2 (12 h).

Table 1
Structure and biological evaluation of the synthesised indole-xanthendione derivatives.

S. No	Code	IC_{50} (T47D) (μM)	IC_{50} ER-alpha binding affinity (nM)	Structure
1	6a	20.9 ± 0.74	355.79 ± 35.37	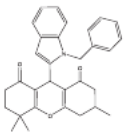
2	6b	19.29 ± 1.93	587.19 ± 58.85	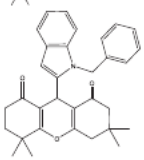
3	6c	19.81 ± 1.03	26.64 ± 2.41	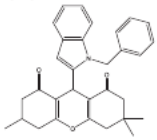
4	6d	23.51 ± 2.81	18.41 ± 1.05	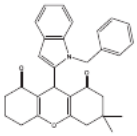
5	**6e**	**16.51 ± 0.75**	**55 ± 1.97**	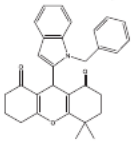
6	**6f**	**17.94 ± 1.0**	**16.55 ± 1.95**	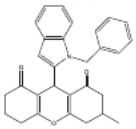
7	6g	24.6 ± 0.07	60.78 ± 0.42	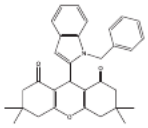
8	6h	ND	ND	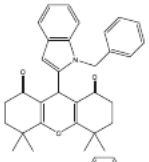
9	6i	ND	ND	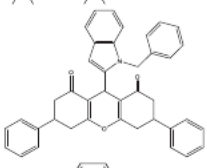
10	6j	ND	482.3 ± 37.44	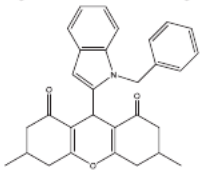
11	6k	25 ± 4.52	51.19 ± 0.67	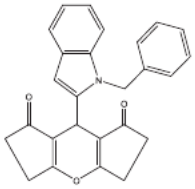

(*continued on next page*)

Table 1 (*continued*)

S. No	Code	IC_{50} (T47D) (μM)	IC_{50} ER-alpha binding affinity (nM)	Structure
12	6l	22.08 ± 2.78	61.08 ± 5.23	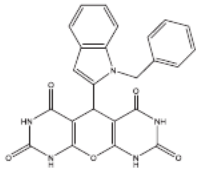
13	6m	ND	ND	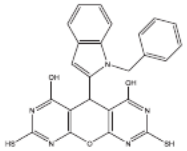
14.	Bazedoxifene	16.43 ± 0.94	31.71 ± 1.41	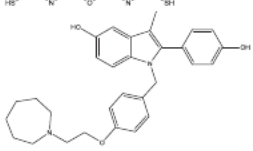

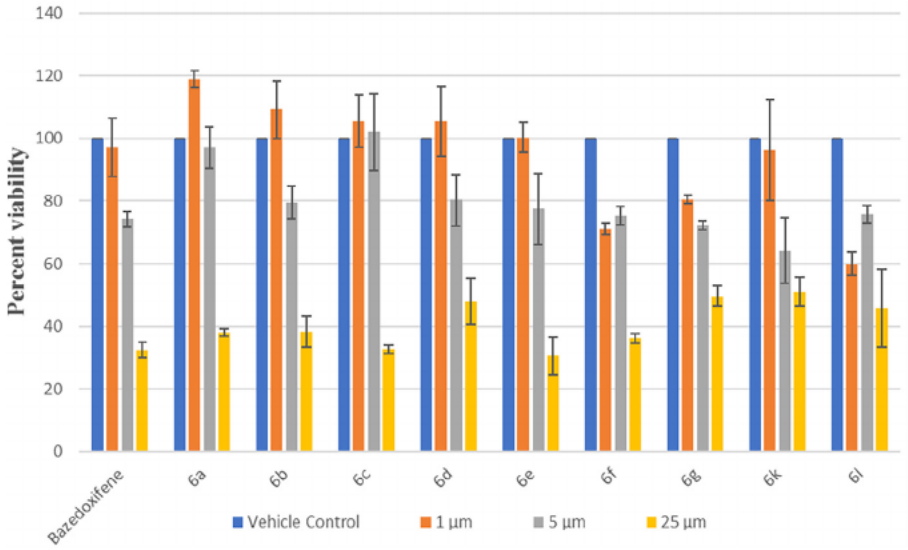

Fig. 2. MTT assay results showing potent and dose dependent anti-proliferative activity of synthesised compounds in comparison to bazedofifene (positive control) on T47D cell line for 48 h.

mechanism but not by targeting ER-α. While other derivatives **6c**, **6d**, **6g**, **6k** and **6l** were having a stronger binding affinity but with a weak anti-proliferative activity. Hence, compounds **6e** and **6f** were selected for further studies as these compounds were showing both impressive antiproliferative activity as well as binding affinity towards the ER-α. Compounds **6e** and **6f** were escalated for confocal laser scanning microscopy (CLSM), RT-PCR and Western blotting for gene expression studies.

It is a known fact that ER-α is distributed in cytoplasm as well as nucleus.[33] In order to identify the cellular distribution of the compounds **6e** and **6f** in T47D cells line CLSM was performed. The compounds **6e** and **6f** has blue emission, therefore DAPI excitation-emission channel was used for their detection in the T47D cells, eliminating the requirement of additional tagging with an fluorochrome. The confocal images indicated selective targeting of cytosol and plasma membrane by the compounds **6e** and **6f** after 24 h incubation at 15 μM respectively. Both the compounds were able to transverse the cellular bio-membrane, but did not enter the nucleus/nucleolus region of T47D cells, hence preventing any possible interaction with the genome at transcription level (Fig. 3). Thus, the confocal images undoubtedly confirm that the compounds are able to interact with the proteins present in the cytosol and plasma membrane. Thereby, obtained results of cell imaging, support our theory of anti-cancer activity displayed by synthesised compounds by targeting cytoplasmic and membrane bound ER-α.

BC progression has been associated with the elevated levels of mRNA for ER-α.[34] A decrease in the mRNA levels can be expected to be observed, if compound under investigation is active and have affinity for ER-α. Therefore, we examined the effect of **6e** and **6f** on the abundance of mRNA of ER-α in human T47D cell lines. The mRNA level of ER-α was determined by RT-PCR using specific primers chosen from human DNA sequences and amplified in simpliAmp thermal cycler (Applied biosystem).

The agarose gel image and the densitometric analysis (Fig. 4) imply that the expression of the mRNA of ER-α was 45.73% and 70.26% in the cells treated with **6e** and **6f** respectively. The results imply that the expression of mRNA was reduced by 54.27% and

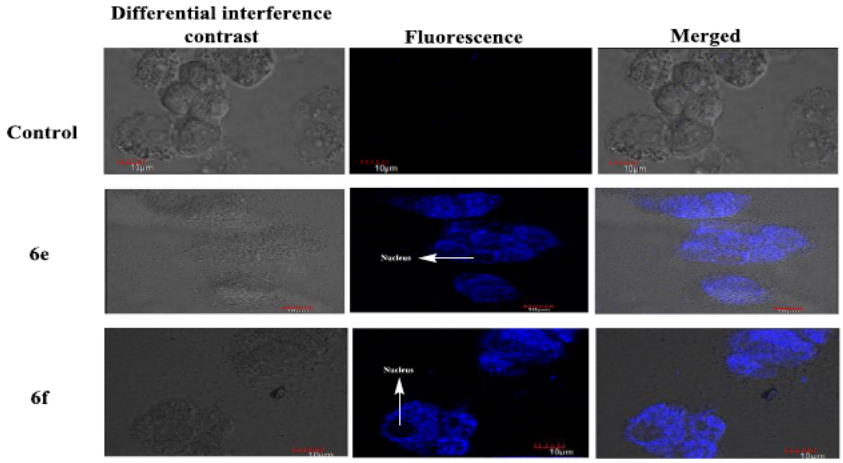

Fig. 3. CLSM analysis of T47D cells after treating the cells with compound **6e** and **6f** for 24 h and untreated cells as a control (Scale bar, 10 μm).

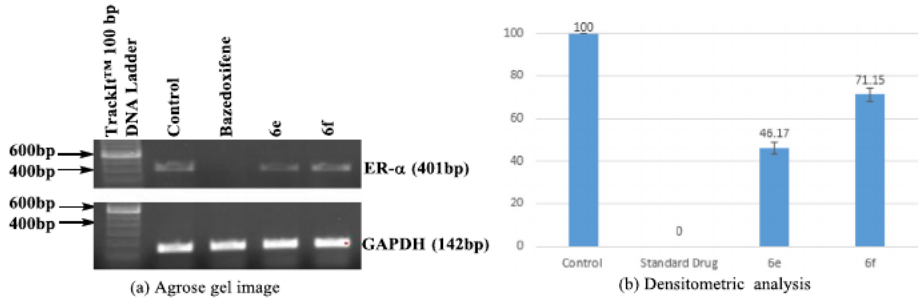

Fig. 4. mRNA expression profile of endogenous ER-α in the T47D cells line after treatment with bazedoxifene and synthesised compounds **6e** and **6f**. The cells were incubated with 15 μM of bazedoxifene, **6e** and **6f** for 48 h. Data was normalised with GAPDH as an internal control, the results shown here are the representatives of three different experiments.

29.74% post treatment with **6e** and **6f** respectively with T47D cell lines as compared to the control (untreated) cells. Thus, it can be concluded that compounds **6e** and **6f** decreases the expression of ER-α at the transcription level, thereby downregulating the signalling and transactivation pathways. ER-α mediated metastasis has been associated with the transactivation of several non-genomic pathways, thereby inhibition of the ER-α protein can lead to enhanced management of BC.[35] In order to quantify the effect of **6e** and **6f** on the expression of ER-α protein, Western blotting was performed. The Western blot image and the densitometry analysis (Fig. 5) shows high levels of ER-α protein in the untreated cells line. In contrast, expression of ER-α protein was reduced by 32.18% and 31.06% in the T47D cells treated with compound **6e** and **6f** respectively (Fig. 5). The results clearly indicate that, compound **6e** and **6f** not only reduces the mRNA expression, but also diminishes the protein levels of ER-α. Thus, it can be concluded that their anticancer activity in T47D cells is by the virtue of targeting the ER-α at the mRNA as well as protein level.

2.3. Structural investigation

Induced fit simulation study was carried out for establishing a structural correlation of compounds **6e** and **6f** with ER-α. Rigid docking protocol is becoming obsolete as it lacks a major factor of protein flexibility which imposes a significant impact on the binding confirmation of the approaching ligand. We have utilised induced fit docking protocol which computes the binding affinity by taking protein flexibility. This protocol reduces the computa-

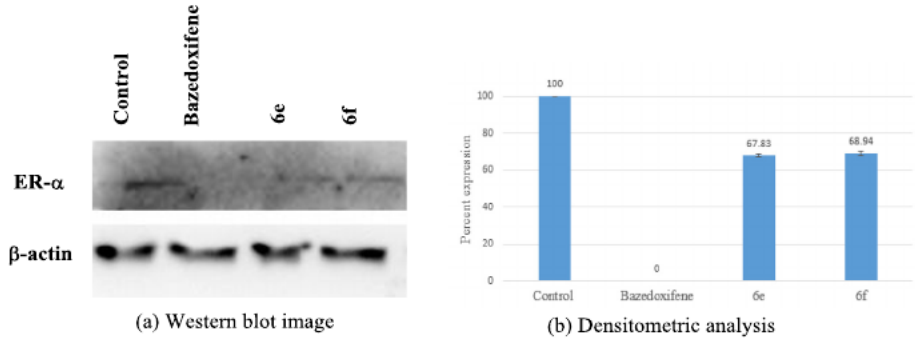

Fig. 5. Western blot analysis of endogenous ER-α protein in the T47D cells after treatment with bazedoxifene, **6e** and **6f**. The cells line was incubated with 15 μM of bazedoxifene, **6e** and **6f** for 48h. Data was normalised with β-actin as internal control, the results shown here are the representatives of three different experiments.

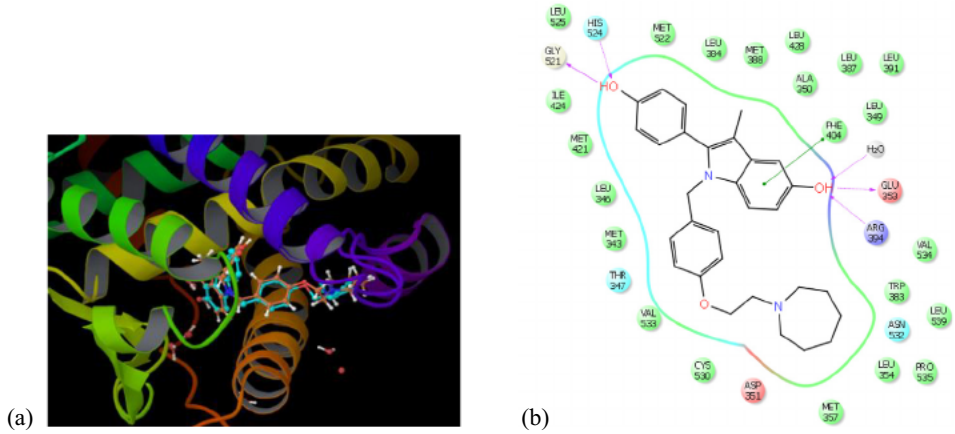

Fig. 6. (a) Superposition of the docked structure of bazedoxifene (blue) with recrystallised experimental pose of bazedoxifene (orange) in 4XI3 with 0.02 Å rmsd (b) Bazedoxifene ligand interaction diagram at the receptor site of ER-α.

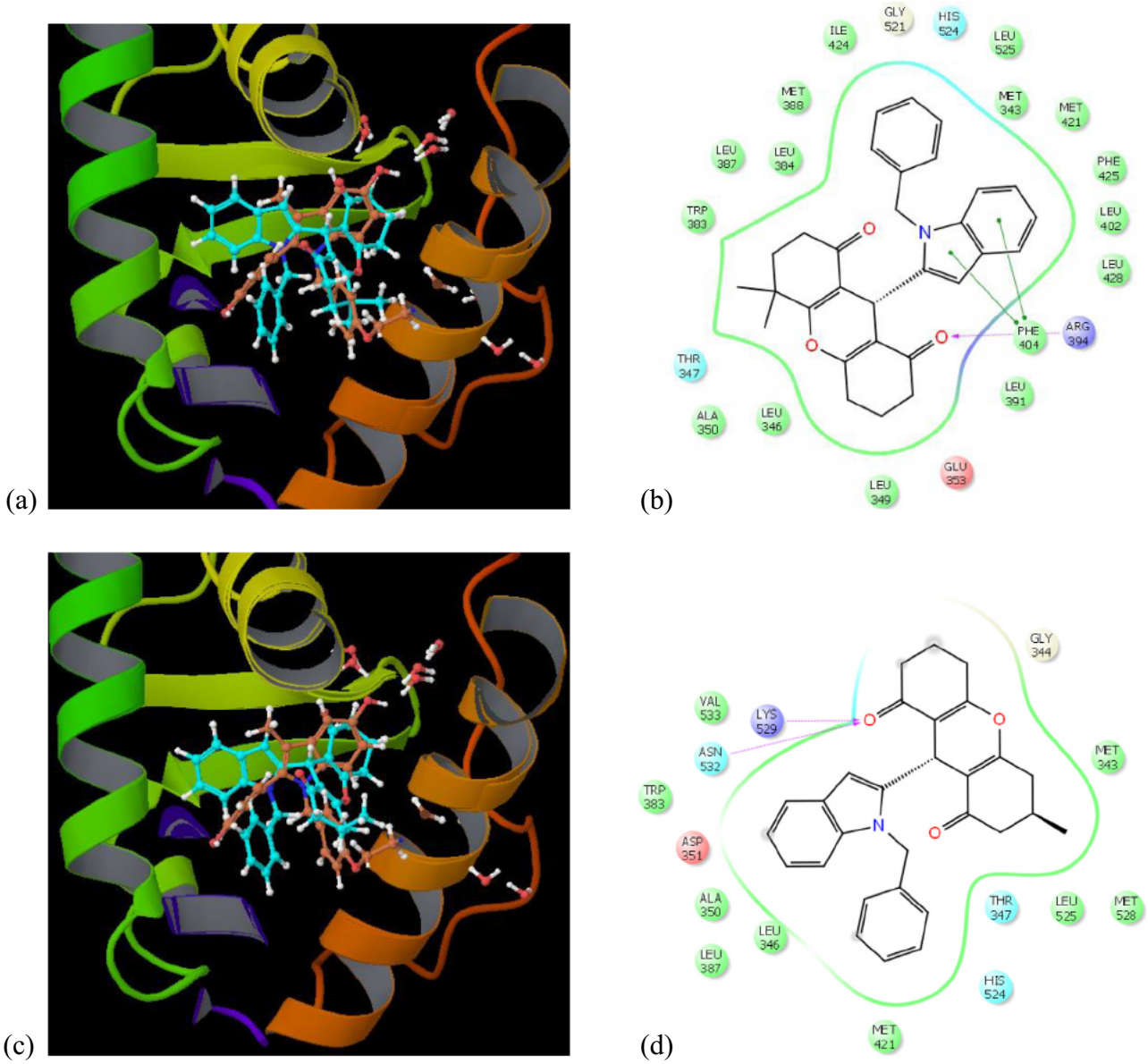

Fig. 7. (a) Superposition of bazedoxifene (brown) with compound **6e** (blue) at receptor site (b) ligand interaction diagram of compound **6e** (c) Superposition of bazedoxifene (brown) with compound **6f** (blue) at receptor site (d) ligand interaction diagram of compound **6f**.

tional time in the prediction of favourable binding mode and conformation of ligand with receptor without compromising with the accuracy.[1]

Docking protocol was validated by redocking the co-crystalized bazedoxifene in their native protein structure (PDB id 4XI3) (Fig. 6a). Upon superimposition of the docked conformation with the experimental co-crystalized bazedoxifene indicates that the docking model reiterates the orientation of the native ligand in the active site with root mean square deviation of 0.02 Å. The interactions observed were retained and consistent with the key amino acids of the binding cavity (Fig. 6a).

The docking pose obtained after the induced fit simulation was analysed and it was observed that, compound **6e** (Fig. 7a, b) and **6f** (Fig. 7c, d) binds to the shallow binding site of the receptor with strong binding affinity of −12.51 kcal/mol and −12.06 kcal/mol respectively as compared to the bazedoxifene (−9.33 kcal/mol). Compound **6e** and **6f** have shown extensive van der Waals forces of interaction with Met 343, Leu 346, Met 421, Ile 424, Leu 525, Met 522, Leu 384, Met 388, Leu 428, Ala 350, Leu 391, Phe 404, Leu 349, Leu 387, Leu 539, Trp 383, Leu 354, Pro 535 and Val 534. The indole moeity of the compounds helps in the anchoring of the xanthendione moiety in the hydrophobic region of the cavity and thereby enabling hydrophobic interaction with the critical amino acids of the binding cavity. The compounds **6e** and **6f**, have shown H-bond interaction with Arg 394 and Lys 529 and Asn 532 respectively. Both the compound interact with the similar amino acids which surrounds in the docking pose of the bazedoxifene. This result in turn indicates that both the compound binds in an antagonistic conformation similar to the bazedoxifene at the receptor site (Fig. 6b), which is a reason behind the comparable affinity obtained for the compound from the ER-α competitor assay performed for these compounds.

The BC proliferation is mediated by the activation and cross talk of ER-α with other growth factor regulators, in the present investigation the lead compounds **6e** and **6f**, inhibit the proliferation of the T47D cells line by acting on the ER-α at the protein as well as at the mRNA level. As the functional integrity of the ER-α is adversely affected by the treatment and it is a known fact that the ER-α is in a dynamic equilibrium in plasma membrane, cytoplasm and nucleoplasm therefore ER-α localised throughout these compartments is sought to be affected. This disruption in the active conformation of ER-α can lead to restriction in the genomic as well as the nongenomic down signalling pathways involved in the BC progression. Moreover, by the initial SAR studies from the biological activity suggest that, presence of alkyl substituents on the xanthedione moiety is beneficial for the activity and bulky substituents like phenyl group as in compound **6i**, should be avoided as it renders the compound inactive. Dimethyl and mono methyl substituents are well tolerated as observed in compounds **6a**, **6b**, **6c**, **6d**, **6e**, **6f** and **6g** but dimethyl substitution should be avoided at 4,4,5,5 position of xanthedione as in compound **6h**. In addition, unsaturated ring system as observed in compound **6m** leads to loss of activity. Docking analysis, indicated that the hit compounds **6e** and **6f** binds to the receptor site in a conformation similar to clinical standard bazedoxifene.

3. Conclusion

In summary, herein we have described the design, synthesis and *in vitro* biological evaluation of novel indole-xanthendione hybrids for targeting ER-α. The indole-xanthendione hybrids initially were screened for the antiproliferative activity, cytotoxicity and ER-α binding affinity. From these studies it was found that, increasing the substitution at the xanthedione moiety decreases the activity and compounds **6e** and **6f** were showing most promising antiproliferative and ER-α binding affinity. Therefore, **6e** and **6f** were escalated for gene expression studies. CLSM experiment indicated that observed anti-proliferative activity of the compounds was likely due to accumulation of compound in cytoplasm and bio membrane. From the RT-PCR and Western blotting it was found that compounds **6e** and **6f** were able to decrease the mRNA and protein expression of the target ER-α, thereby decreasing the ER-α activity. Induced fit docking assisted in extracting the structural attributes behind the promising *in vitro* biological activity of the compounds **6e** and **6f**. Both the compounds form extensive hydrophobic and hydrogen bond interaction with the similar amino acids neighboring the bazedoxifene hence, binds in the antagonistic confirmation similar to bazedoxifene. The result obtained the study is encouraging considering that compound **6e** and **6f** represents example of an indole-xanthendione derivatives could be used in future *in vivo* testing as a potent compound for the management of BC.

4. Experimental

4.1. Chemistry

4.1.1. General information

Starting materials and solvents were purchased from commercial suppliers and used without further purification. Reaction progress was monitored by TLC using silica gel 60 F254 (0.040e0.063 mm) with detection by UV. Silica gel 60–120 and 200–400 was used for column chromatography and flash chromatography respectively. Yields refer to purified materials and are not optimized. ^{1}H NMR and ^{13}C NMR spectra were recorded on a Jeol 400 MHz and Bruker 400 MHz spectrometer using the residual signal of the deuterated solvent as internal standard. Splitting patterns are described as singlet (s), doublet (d), triplet (t) and broad (br); chemical shifts (d) are given in ppm. High-resolution mass spectra (HRMS) were recorded on an Q-ToF Micro Waters. Melting points were recorded on Stuart melting point apparatus (SMP-30) with open glass capillary tube and were uncorrected.

4.1.2. General procedure for the synthesis of intermediates 2,3,4 and 5

Potassium hydroxide (4 mmol) was stirred in dried dimethyl sulfoxide (25 mL) for 10 min in a round-bottom flask. Ethyl 1*H*-indole-2-carboxylate **1** (1 mmol) was added to the solution and the mixture was stirred for 0.5 h. Benzyl bromide (1.3 mmol) was added to the stirring mixture. After the completion of the reaction (1.5 h) as monitored by TLC the reaction mixture was cooled to 0 °C. Product was extracted with ethyl acetate, the organic layer was washed using brine solution (40 mL). The combined organic layer was dried over anhydrous sodium sulfate, filtered, concentrated and was purified by isocratic flash column chromatography (petroleum ether: ethyl acetate = 9:1, v/v) on silica gel (200–400) to get pure compound **2** with 95% yield.

For the synthesis of **3**, lithium aluminium hydride (2 mmol) was stirred in dry THF at 0 °C. Then **2** (1 mmol) was dissolved in THF and added drop wise to the solution of lithium aluminium hydride at 0 °C. Then, the mixture was slowly warmed to room temperature till the completion (0.5 h) of reaction as monitored by TLC. It was then cooled to 0 °C, 10% aqueous sodium hydroxide (20 mL) and 40 mL of water was added successively. Then reaction mixture was allowed to stir for 0.5 h, filtered through Celite and washed with dry ethyl acetate, dried over anhydrous sodium sulfate, concentrated and purified by isocratic flash column chromatography (petroleum ether: ethyl acetate = 8:2, v/v) on silica gel (200–400) to get pure compound **3** with 98% yield.

For the synthesis of **4**, compound **3** (1 mmol) was dissolved in dry CH_2Cl_2 (25 mL) was stirred briefly. Activated manganese diox-

ide (7.3 mmol) was added, stirred at room temperature for 4 h. Another portion of activated manganese dioxide (5.9 mmol) was added and stirred at room temperature for 0.5 h. After completion of the reaction, as monitored by TLC, the reaction mixture was filtered through Celite and washed with ethyl acetate, concentrated and purified by isocratic flash chromatography (petroleum ether: ethyl acetate 9.5:0.5, v/v) on silica gel (200–400) to afford pure compound **4** with 70% yield.

For the synthesis of **5**, a mixture of compound **4** (1 mmol), corresponding dimedone (2 mmol) and PEG 6000 (5 mol%) in distilled water was subjected to open vessel microwave irradiation at 90 °C, automatic power output for 2.5 h. After completion of the reaction, as monitored by TLC, the solid compound **5** obtained was washed secretively with water and dried *in vacuo* for removing any residual water content. Compound was purified by isocratic flash chromatography (petroleum ether: ethyl acetate 8.5:1.5, v/v) on silica gel (200–400) to afford pure compound **5** with 95% yield.

4.1.3. General procedure for the synthesis of compounds 5

For the synthesis of **6a-m**, compound **5** (1 mmol) was dissolved in dry CH_2Cl_2 (25 mL) was stirred briefly. The DCC (10 mol%) was added and stirred at room temperature for 12 h. After completion of the reaction, as monitored by TLC, compound was purified by isocratic flash chromatography (petroleum ether: ethyl acetate 8.5:1.5, v/v) on silica gel (200–400) to afford pure compound **6a-m** with 56–85% yields.

*4.1.3.1. 9-(1-benzyl-1H-indol-2-yl)-3,5,5-trimethyl-3,4,5,6,7,9-hexahydro-1H-xanthene-1,8(2H)-dione (**6a**).* Pale white solid; yield 56%; mp 251–253 °C; ^{1}H NMR (400 MHz, DMSO d_6 + $CDCl_3$) δ 8.14–8.12 (1H, d, *J = 8 Hz*), 8.07–8.06 (1H, d, *J = 4 Hz*), 7.38–7.32 (2H, m), 7.26–7.20 (6H, m), 5.63 (2H, s), 5.49 (1H, s), 3.23 (6H, s), 2.53–2.44 (2H, m), 2.39–2.14 (2H, m), 2.01–1.71 (2H, m), 1.40–1.18 (2H, m),1.09–0.87 (4H, m). ^{13}C NMR (100 MHz, DMSO + $CDCl_3$) δ 197.00 (2C), 173.69, 142.75, 142.41, 137.35, 136.15, 128.29 (2C), 126.98, 126.34 (2C), 125.16, 121.82, 120.96, 119.46, 112.10, 108.39, 107.96, 97.76, 47.77, 46.00, 45.21, 44.71, 37.00, 29.09, 27.74, 27.49, 21.14 (2C), 20.90. HRMS(ESI):*m/z* calcd for $C_{31}H_{32}NO_3^+$ $[M+H]^+$ 466.2382; found: 466.2380.

*4.1.3.2. 9-(1-benzyl-1H-indol-2-yl)-3,3,5,5-tetramethyl-3,4,5,6,7,9-hexahydro-1H-xanthene-1,8(2H)-dione (**6b**).* Off white solid; yield 70%; mp 251–252 °C; ^{1}H NMR (400 MHz, DMSO d_6 + $CDCl_3$) δ 8.20–8.18 (1H, d, *J = 8 Hz*), 7.88–7.86 (1H, d, *J = 8 Hz*), 7.31–7.27 (7H, m), 5.71 (2H, s), 5.60 (1H, s), 2.53–2.51 (3H, m), 2.40–2.36 (2H, m), 2.14–1.71 (4H, m), 1.25 (6H, s), 0.91 (6H, s). ^{13}C NMR (100 MHz, DMSO d_6 + $CDCl_3$) δ 197.43 (2C), 172.26, 142.21, 141.21, 136.15, 135.06, 128.39 (2C), 128.04, 126.61 (2C), 125.62, 121.44, 119.67, 118.38, 111.26, 109.00, 108.36, 98.19, 50.41, 47.67, 45.79, 44.62, 42.78, 30.89 (2C), 29.46 (2C), 28.56 (2C), 24.97. HRMS (ESI):*m/z* calcd for $C_{32}H_{34}NO_3^+$ $[M+H]^+$ 480.2539; found: 480.2538.

*4.1.3.3. 9-(1-benzyl-1H-indol-2-yl)-3,3,6-trimethyl-3,4,5,6,7,9-hexahydro-1H-xanthene-1,8(2H)-dione (**6c**).* Off white solid; yield 74%; mp 182–184 °C; ^{1}H NMR (400 MHz, DMSO d_6 + $CDCl_3$) δ 7.89–7.84 (2H, m), 7.65–7.60 (1H, m), 6.85–6.80 (6H, m), 6.64–6.62 (1H, m), 5.39 (2H, s), 5.30 (1H, s), 2.26–2.20 (3H, m), 2.07–2.03 (2H, m), 1.87–1.47 (3H, m), 1.00 (2H, s), 0.80–0.75 (6H, m), 0.65 (2H, s).^{13}C NMR (100 MHz, DMSO d_6 + $CDCl_3$) δ 196.07(2C), 161.45, 142.29, 141.20, 138.11, 137.45, 136.12, 128.32 (2C), 127.90, 126.41 (2C), 125.21, 121.35, 119.53, 118.34, 112.01, 111.36, 108.09, 97.98, 50.18, 47.85, 47.67, 45.94, 44.52, 30.80, 29.43, 28.61, 23.60, 20.24. HRMS (ESI):*m/z* calcd for $C_{31}H_{32}NO_3^+$ $[M+H]^+$ 466.2382; found: 466.2381.

*4.1.3.4. 9-(1-benzyl-1H-indol-2-yl)-3,3-dimethyl-3,4,5,6,7,9-hexahydro-1H-xanthene-1,8(2H)-dione (**6d**).* Off white solid; yield 64%; mp 247–248 °C; ^{1}H NMR (400 MHz, $CDCl_3$) δ 8.05–8.01 (1H, m), 7.22–7.15 (8H, m), 7.06–7.02 (1H, m), 5.53 (2H, s), 5.46 (1H. s), 2.51–2.47 (1H, m), 2.33–2.22 (2H, m), 1.76–1.71 (1H, m), 1.38–1.32 (2H, m), 1.24–1.22 (4H, m), 1.18 (6H, s). ^{13}C NMR (100 MHz, $CDCl_3$) δ 197.54 (2C), 171.34, 143.50, 142.02, 138.15, 137.25, 128.87 (2C), 127.51, 126.50 (2C), 125.62, 121.79, 119.97, 119.29, 113.05, 109.38, 108.64, 100.29, 50.78, 48.93, 41.06, 31.12 (2C), 29.72, 29.65 (2C), 29.47, 22.71. HRMS (ESI):*m/z* calcd for $C_{30}H_{30}NO_3^+$ $[M+H]^+$ 452.2226; found: 452.2225.

*4.1.3.5. 9-(1-benzyl-1H-indol-2-yl)-4,4-dimethyl-3,4,5,6,7,9-hexahydro-1H-xanthene-1,8(2H)-dione (**6e**).* Pale yellow solid; yield 69%; mp 293–294 °C; ^{1}H NMR (400 MHz, $CDCl_3$) δ 8.06–8.04 (2H, d, *J = 8 Hz*), 8.02–8.01 (2H, d, *J = 4 Hz*), 7.32–7.26 (6H, m), 5.65 (1H, s), 5.55 (2H, s), 2.57–2.47 (2H, m), 1.96–1.87 (2H, m), 1.74–1.65 (2H, m), 1.33–1.32 (2H, m), 1.27–1.26 (2H, m), 1.21–1.18 (6H, m). ^{13}C NMR (100 MHz, $CDCl_3$) δ 197.14 (2C), 177.17, 142.98, 142.05, 137.99, 137.25, 128.86 (2C), 127.49, 126.50 (2C), 125.43, 121.62, 119.93, 119.10, 112.55, 109.36, 108.61, 100.27, 48.35, 46.79, 40.60, 35.29 (2C), 34.41, 29.71, 25.43 (2C), 24.51. HRMS (ESI):*m/z* calcd for $C_{30}H_{30}NO_3^+$ $[M+H]^+$ 452.2226; found: 452.2225.

*4.1.3.6. 9-(1-benzyl-1H-indol-2-yl)-3-methyl-3,4,5,6,7,9-hexahydro-1H-xanthene-1,8(2H)-dione (**6f**).* Pale white solid; yield 70%; mp 258–259 °C; ^{1}H NMR (400 MHz, $CDCl_3$) δ 8.06–8.04 (1H, d, *J = 8 Hz*), 8.00–7.99 (1H, d, *J = 8 Hz*), 7.22–7.16 (6H, m), 7.03–6.91 (2H, m), 5.51 (2H, s), 5.35 (1H, s), 2.66–2.44 (2H, m), 2.34–2.12 (2H, m), 2.00–1.94 (1H, m), 1.21–1.16 (6H, m), 1.04–1.00 (3H, m). ^{13}C NMR (100 MHz, $CDCl_3$) δ 198.00 (2C), 172.95, 143.34, 143.77, 138.56, 137.27, 128.86 (2C), 127.50, 126.51 (2C), 125.18, 121.70, 119.26, 118.77, 113.66, 108.93, 108.63, 100.15, 48.66, 46.77, 45.67, 36.11, 35.37, 31.95, 29.72, 28.18, 22.71. HRMS (ESI):*m/z* calcd for $C_{29}H_{27}NO_3^+$ $[M]^+$ 437.1991; found: 437.1990.

*4.1.3.7. 9-(1-benzyl-1H-indol-2-yl)-3,3,6,6-tetramethyl-3,4,5,6,7,9-hexahydro-1H-xanthene-1,8(2H)-dione (**6g**).* Pale yellow solid; yield 57%; mp 153–154 °C; ^{1}H NMR (400 MHz, $CDCl_3$) δ 7.58–7.55 (1H, m), 7.29–7.25 (2H, m), 7.22–7.19 (1H, m), 7.09–7.05 (3H, m), 6.93–6.91 (2H, d, *J = 8 Hz*), 6.47 (1H, s), 5.54 (1H, s), 5.13 (2H, s), 2.20 (4H, s), 2.05–2.00 (2H, m), 1.82–1.78 (2H, m), 0.95 (12H, s).^{13}C NMR (100 MHz, $CDCl_3$) δ 197.49 (2C), 171.32 (2C), 142.00, 137.22, 136.32, 128.84 (2C), 128.65, 126.48 (2C), 125.60, 121.76, 119.94, 119.26, 113.05 (2C), 108.61, 99.96, 50.77, 48.90 (2C), 46.74 (2C), 41.06 (2C), 31.62, 31.09, 29.69, 29.62, 29.45. HRMS (ESI):*m/z* calcd for $C_{32}H_{34}NO_3^+$ $[M+H]^+$ 480.2539; found: 480.2538.

*4.1.3.8. 9-(1-benzyl-1H-indol-2-yl)-4,4,5,5-tetramethyl-3,4,5,6,7,9-hexahydro-1H-xanthene-1,8(2H)-dione (**6h**).* Red viscous liquid; yield 77%; bp 221–222 °C; ^{1}H NMR (400 MHz, $CDCl_3$) δ 7.45–7.43 (1H, m), 7.33–7.27 (4H, m), 7.25–7.23 (1H, m), 6.98–6.95 (3H, m), 6.16 (1H, s), 5.83 (2H, s), 4.92 (1H, s), 2.47 (4H, s), 2.24–2.14 (4H, m), 1.09 (6H, s), 1.04 (6H, s). ^{13}C NMR (100 MHz, $CDCl_3$) δ 196.55 (2C), 162.16 (2C), 145.09, 138.35, 136.81, 128.31 (2C), 127.96, 127.13 (2C), 126.80, 120.88, 119.71, 119.26, 115.20 (2C), 111.20, 100.84, 50.71, 47.99 (2C), 41.01 (2C), 32.21 (2C), 29.73, 29.06 (2C), 27.69 (2C). HRMS (ESI):*m/z* calcd for $C_{32}H_{34}NO_3^+$ $[M+H]^+$ 480.2539; found: 480.2538.

*4.1.3.9. 9-(1-benzyl-1H-indol-2-yl)-3,6-diphenyl-3,4,5,6,7,9-hexahydro-1H-xanthene-1,8(2H)-dione (**6i**).* Pale yellow solid, yield 63%, mp 208–209 °C; ^{1}H NMR (400 MHz, $CDCl_3$) δ 7.50–7.47 (1H, m), 7.36–7.31 (3H, m), 7.29–7.24 (7H, m), 7.21–7.14 (5H, m), 7.03–6.99 (3H, m), 6.24–6.21 (1H, m), 5.84–5.63 (2H, m), 5.11 (1H, s), 3.46–3.40 (1H, m), 3.25–3.17 (1H, m), 2.87–2.79 (4H, m), 2.67–

2.45 (4H, m). ^{13}C NMR (100 MHz, $CDCl_3$) δ 195.74, 195.51, 162.67, 162.46, 142.05, 142.02, 141.97, 138.43, 137.06, 128.93 (2C), 128.89 (2C), 128.88 (2C), 128.43, 127.30 (2C), 126.83 (2C), 126.75 (2C), 126.73 (2C), 126.67, 121.24, 119.86, 119.59, 116.25, 116.03, 110.91, 101.70, 47.62, 43.93, 43.70, 38.83, 37.89, 34.93, 34.89, 24.23. HRMS (ESI):*m*/*z* calcd for $C_{40}H_{34}NO_3^+$ $[M+H]^+$ 576.2539; found: 576.2538.

*4.1.3.10. 9-(1-benzyl-1H-indol-2-yl)-3,6-dimethyl-3,4,5,6,7,9-hexahydro-1H-xanthene-1,8(2H)-dione (**6j**).* pale yellow solid; yield 58%; mp 218–219 °C; ^{1}H NMR (400 MHz, $CDCl_3$) δ 7.49–7.47 (1H, d, *J* = *8 Hz*), 7.18–7.13 (4H, m), 7.00–6.93 (3H, m), 6.83–6.79 (2H, m), 5.45 (1H, s), 5.06 (2H, s), 2.38–2.20 (4H, m), 1.93–1.85 (4H, m), 1.20–1.18 (2H, m), 0.82–0.79 (6H, m).^{13}C NMR (100 MHz, $CDCl_3$) δ 189.76 (2C), 167.10 (2C), 137.01, 136.63, 135.90, 127.66 (2C), 125.93, 124.56 (2C), 124.52, 120.48, 119.14, 118.78, 115.29 (2C), 108.50, 101.60, 45.91, 40.80 (2C), 39.82 (2C), 27.15, 27.06, 25.53 (2C), 19.37. HRMS (ESI):*m*/*z* calcd for $C_{30}H_{30}NO_3^+$ $[M+H]^+$ 452.2226; found: 452.2225.

*4.1.3.11. 8-(1-benzyl-1H-indol-2-yl)-3,5,6,8-tetrahydro-1H-dicyclopenta[b,e]pyran-1,7(2H)-dione (**6k**).* Pale white solid; yield 61%; mp 219–220; ^{1}H NMR (400 MHz, DMSO d_6 + $CDCl_3$) δ 7.43–7.41 (1H, d, *J* = *8 Hz*), 7.28–7.20 (5H, m), 7.15–7.13 (1H, d, *J* = *8 Hz*), 7.02–6.95 (2H, m), 6.19 (1H, s), 5.71 (2H, s), 4.65 (1H, s), 3.44–3.30 (4H, m), 2.86–2.75 (4H, m). ^{13}C NMR (100 MHz, DMSO d_6 + $CDCl_3$) δ 201.02 (2C), 177.59, 156.96, 140.05, 137.70, 136.38, 128.07 (2C), 127.21, 126.64 (2C), 126.06, 120.93, 119.64, 119.23, 118.56 (2C), 109.60, 101.12, 47.59, 33.70 (2C), 33.41 (2C), 25.25. HRMS (ESI):*m*/*z* calcd for $C_{26}H_{22}NO_3^+$ $[M+H]^+$ 396.1600; found: 396.1599.

*4.1.3.12. 5-(1-benzyl-1H-indol-2-yl)-5,9-dihydro-2H-pyrano[2,3-d:6,5-d']dipyrimidine 2,4,6,8(1H,3H,7H)-tetraone (**6l**).* Red solid; yield 85%; mp 268–269 °C; ^{1}H NMR (400 MHz, DMSO d_6 + $CDCl_3$) δ 8.77 (1H, s), 8.46 (1H, s), 7.78–7.76 (1H, d, *J* = *8 Hz*), 7.66–7.64 (1H, d, *J* = *8 Hz*), 7.40–7.36 (1H, t, *J* = *8 Hz*), 7.29–7.22 (4H, m), 7.17–7.13 (1H, t, *J* = *8 Hz*), 7.07–7.05 (2H, d, *J* = *8 Hz*), 5.71 (2H, s), 3.34 (1H, s), 2.51 (2H, s). ^{13}C NMR (100 MHz, DMSO d_6 + $CDCl_3$) δ 163.59 (2C), 161.80 (2C), 150.05 (2C), 140.42, 138.87, 137.61, 128.62 (2C), 127.62, 126.83, 126.06 (2C), 123.23, 121.17, 117.87, 114.09, 111.05 (2C), 99.05, 45.94, 45.88. HRMS (ESI):*m*/*z* calcd for $C_{24}H_{18}N_5O_5^+$ $[M+H]^+$ 456.1308; found: 456.1307.

*4.1.3.13. 5-(1-benzyl-1H-indol-2-yl)-2,8-dimercapto-2,3,5,7,8,9-hexahydro-4H-pyrano[2,3-d:6,5-d']dipyrimidine-4,6(1H)-dione (**6m**).* Red solid; yield 80%; mp 193–194 °C; ^{1}H NMR (400 MHz, DMSO d_6 + $CDCl_3$) δ 11.54 (1H, br), 8.49 (1H, s), 7.78–7.66 (1H, m), 7.40–6.90 (8H, m), 6.32–6.19 (1H, m), 5.72 (2H, s), 5.23 (1H, s), 2.52 (2H, s). ^{13}C NMR (100 MHz, DMSO d_6 + $CDCl_3$) δ 177.94 (2C), 172.70 (2C), 161.93 (2C), 140.94, 139.49, 137.69, 128.73 (2C), 127.51, 126.12 (2C), 125.65, 123.51, 121.46, 118.76, 114.16, 111.30 (2C), 95.13, 45.95, 45.90. HRMS (ESI):*m*/*z* calcd for $C_{24}H_{18}N_5O_3S_2^+$ $[M+H]^+$ 488.0851; found: 488.0854.

4.2. Biological assay methods

4.2.1. Culturing and maintaining of cancer cell line

Human BC cell line T47D were procured from National Centre for Cell Sciences (NCCS) Pune. T47D cells were grown in the Roswell Park Memorial Institute-1640 (RPMI-1640) medium supplemented with 10% heat inactivated (30 min at 56 °C) FBS (Fetal Bovine Serum), 1X penicillin and streptomycin in a tissue culture flask at 37 °C in a humidified atmosphere of 5% CO_2 incubator. At 70–80% confluence the cells were trypsinized using 1X trypsin-EDTA and sub-cultured in a new sterile tissue culture flask for further experiments.

4.2.2. Anti-proliferative activity

The anti-proliferative activity of the compounds was evaluated using the MTT assay. It is a colorimetric assay for assessing cell metabolic activity. Viable cells with active metabolism convert the MTT into a purple coloured formazan product with an absorbance maximum near 570 nm. When cells die, they lose the ability to convert MTT into formazan, thus color formation serves as a useful and convenient marker of only the viable cells. Human BC cell line T47D were seeded in 96 wells plate at cell density 1×10^4 per well and after 24 h, cells were treated with different concentration of synthesised compounds (1, 5, 25 μM) and incubated for 48 h in FBS-free media. MTT solution (final concentration of MTT was 0.5 mg/ml) was added followed by incubation for 4 h at 37 °C. After 4 h; the purple color farmazone crystals were solubilized using 100 μL of acidified DMSO with 0.6% acetic acid and absorbance was measured at both 570 nm and 620 nm. The absorbance reading is directly proportional to a number of living cells.[36] The cell viability of each group was calculated with their respective control.

4.2.3. Human peripheral blood mononuclear cells (PBMCs) culture and MTT assay

Majority of the chemotherapeutic agents available having a side effect of inducing apoptosis in the normal cell along with the cancer cells. Therefore, in order to analyze the side effect of the compounds on the normal cells at higher concentrations, human PBMC was cultured and MTT assay was performed. Fresh blood was drawn from healthy individual as per the protocol No. CUPB/cc/14/IEC/4483 approved by Institutional Ethics Committee of Central University of Punjab, Bathinda. The protocol used was standard operating procedure, provided by Institutional Ethics Committee of Central University of Punjab according to guidelines issued by Indian Council of Medical Research (ICMR), Govt. of India. PBMC were isolated from whole blood discarding the RBCs after treatment with RBC lysis buffer. The PBMCs were counted on the automated cell counter (Invitrogen). The cells were then suspended in RPMI-1640 media supplemented with 10% fetal bovine serum (FBS), 1 × antibiotic solution and incubated at 37 °C in a humidified atmosphere of 5% CO_2. Approximately 10^4 cells were seeded in each well of the 96 well plate. MTT assay was performed as described in section 4.2.2.

4.2.4. Estrogen receptor competitive binding assay

A stock solution of each compound was serially diluted using DMSO, and the 40 μL of each concentration was transferred to the assay plate (Grenier, 384-well high volume flat bottom) followed by adding 40 μL human recombinant ER-α/fluoromone TM complex solution. After mixing and allowing at least 2 h incubation at room temperature with light protection of the reagents. The fluorescence of each well was measured using the Synergy 2 multimode microplate reader (BioTek) with 535 nm excitation filters and 590 nm emission filters. Three controls were included in the assay: (1) assay maximum polarization control (40 μL of ER/fluoromone complex solution and 40 μL of ER green assay buffer with 4% DMSO, provides maximum polarization value for assay); (2) assay minimum polarization control (40 μL of ER/fluromone complex solution and 40 μL of oestradiol (20 mM), provides bottom baseline); (3) free fluoromone tracer control (40 μL Fluoromone tracer and 40 μL of ER green assay buffer with 4% DMSO, provides absolute minimum polarization value). The polarization values were normalised to percent inhibition using the following equation.

$$I\% = (A_0 - A)/(A_0 - A_{100}) \times 100$$

I% = the percent inhibition, A_0 = Absorbance at 0% inhibition, A_{100} = Absorbance at 100% inhibition, and A = observed Absorbance value.

The percent inhibition values are plotted against the concentration of test compounds and analysed by a non-linear regression curve fitting. The concentration of the test compounds needed to displace half of the bond ligand equals IC_{50} of the test compound.

4.2.5. Confocal microscopy

Cell imaging is an important technique for locatisation of the compound inside the cell. As the ER is located on the plasma membrane, cytosol and nucleoplasm, live cell imaging enables to track the compound and site of action. Cells were seeded on sterile glass coverslip at 5×10^4 cells/ml in a 6 wells plate. After 24 h of seeding the cells were treated with 15 μM of **6e** and **6f** for 48 h after that cells were washed with 1X PSB. After that cells were fixed with 2% formaldehyde solution for 10 min in dark, again cells were washed thrice with 1X PBST. Then cells were mounted on glass cover by using mounting media. Cells were visualized and image was captured under an Olympus FV1200 Laser Scanning Microscopes fluorescence confocal microscope, the captured image was analysed with Olympus Fluoview software of Olympus version 4.2a.

4.2.6. Preparation of total cell lysates

To determine target specificity of the compounds, there is a need to determine the expression of target proteins. Cell lysates were prepared from both treated and untreated cells of T47D Briefly, cells were first rinsed twice gently with ice-cold 1X PBS, then 300–500 μL of modified RIPA buffer [50 mM TrisHCl (pH 7.4), 150 mM NaCl, 1 mM EDTA, 1% NP-40, and protease inhibitor cocktail (1 μL per 100 μL of lysis buffer)] was added per plate, kept on ice for 5 min, and cells were mechanically scraped using plastic cell scraper and cell suspension was transferred into pre-cooled 1.5 mL micro centrifuge tube.[37] Following centrifugation, the pellet was re-suspended in the cell lysis buffer with intermediate vortexing every 5 min for 20 min at 4 °C. Then, the mixture was centrifuged at 12,000*g* for 20 min at 4 °C. The supernatant was collected in prechilled sterile micro centrifuge tubes and stored at −20 °C for further experiments. The concentration of total protein in this supernatant was estimated by using standard Bradford method with BSA as standard.[38]

4.2.7. Western blot analysis

50 μg of total protein sample were resolved on 10% denaturation SDS-PAGE and transferred to a nitrocellulose membrane. Membranes were blocked for 1 h with 5% nonfat dry milk (NFDM) in 1X PBST. All antibody dilutions were made in 2.5% NFDM-PBST. Membranes were incubated (4°C overnight) with primary antibodies of rabbit α-ER- α (HC-20. Membranes were washed with PBST, incubated with horseradish peroxidase-conjugated secondary antibody (Invitrogen) for 1 h. The image was captured by by using Bio-Rad ChemiDoc™ MP imaging system after applying enhanced chemiluminescence (Clarity™ Western ECL Substrate of Bio-Rad) and densitometric analysis was done using Image Lab™ software of Bio-Rad version 5.2.

4.2.8. Total RNA Isolation and cDNA synthesis

Total RNA was isolated from T47D cells from both treated and untreated cells by using TRIzol® (Invitrogen), and followed the manufacturer instructions and finally RNA pellet was resuspended in nuclease free water. Quality of isolated RNA was checked on NanoDrop 2000c (Thermo Scientific) followed by denaturing agarose gel. Traces of DNA contamination was removed by treating the total isolated RNA with DNA-free™ DNA Removal Kit (Invitrogen), and followed the manufacturer instructions. Again, the quality of DNA free RNA was checked, followed by synthesis of first strand of cDNA by using the SuperScript™ IV First-Strand Synthesis System (Invitrogen) as per the instructions by the manufacturer.

4.2.9. RT-PCR

cDNA was used as a template for the PCR reaction with gene-specific primer pairs of ER-α (5′ GTGCCTGGCTAGAGATCCTG 3′, 3′ GATGTGGGAGAGGATGAGGA 5′) along with a housekeeping gene (GAPDH) as a loading control. The PCR product was separated on 1.2% agarose gel containing ethidium bromide (EtBr) along with 100 bp DNA ladder of Invitrogen (Tracklt™ 100 bp DNA ladder). The gel image was taken by using Bio-Rad Gel Doc™ XR system and densitometric analysis was done using Image Lab™ software of Bio-Rad version 5.2.

4.3. Induced fit docking

The 2D structure of ligands were constructed using the maestro 9.6 software and saved in sdf format (standard data format). The 2D structures were converted to the 3D structure using the Ligprep module of Maestro 9.6. This module adds hydrogens, eliminates any discrepancies between bond length and angle. The 3-dimentional and X-ray structure coordinates of ER-α was obtained from protein data bank with PDB id code 4XI3 (www.rcsb.org). Protein preparation wizard of maestro 9.6 was used for the protein preparation. Protein preparation begins with the application of Impact molecular mechanics program for correcting the bond orders, adding missing hydrogens and removing the crystallized waters that are not present in the active site.

A Truncated Newton Conjugate Gradient (TNCG) minimization was performed using the OPLS-2005 force field. IFD protocol utilizes a combination of Glide (grid-based ligand docking with energetics) rigid docking and prime (protein structure prediction). IFD consisted of three-step procedure for sampling side chain conformations and predicting ligand-residue orientations. In the first step, side chain conformation is generated, all previously mutated side chains were back mutated concurrently into a random rotamer state obtained from the rotamer libraries developed by Xiang and Honig. In the second step after the conformation generation, each side chain is minimized successively (<0.001 kcal mol rms gradient) while all other side chains are remaining fixed. Minimization of individual side chains was repeated sequentially for all back mutated residues until convergence was reached. In the third step, a TNCG minimization performed to resolve steric clashes. The target substrates obtained after the final step within a 40 kcal/mol window were redocked into the induced fit structures. GlideXP (Glide Extra precision) with vdW scaling 0.8 was employed for all docking. 20 poses were requested for the redocking and ranked based on the GlideXP score. Application of the IFD protocol produced an individual ensemble for ER-α complexes, which clustered for each compound under investigation. The cluster for the top scoring indole alkaloid was analysed.

Acknowledgements

Authors are grateful to Department of Science and Technology, New Delhi, India for providing financial assistance during the course of the work. Ramit Singla acknowledge CSIR-India for the award of SRF. Authors acknowledge Mr. Ashish Pandey of CIL in Central University of Punjab, for outstanding work on CLSM. Authors are also thankful to the Honourable Vice-Chancellor for providing the necessary facilities at Central University of Punjab, Bathinda, India.

A. Supplementary data

Supplementary data associated with this article can be found, in the online version, at https://doi.org/10.1016/j.bmc.2017.11.040.

References

1. Singla R, Jaitak V. Multitargeted molecular docking study of natural-derived alkaloids on breast cancer pathway components. *Curr Computer-Aided Drug Des*. 2017;13. ahead of print.
2. Singh JS, Singla R, Sharma M, Jaitak V. Indole derivatives as anticancer agents for breast cancer therapy: a review. *Anti-Cancer Agents Med Chem Anti-Cancer Agents*. 2016;16:160–173.
3. Kelly PM, Bright SA, Fayne D, et al. Synthesis, antiproliferative and pro-apoptotic activity of 2-phenylindoles. *Bioorg Med Chem*. 2016;24:4075–4099.
4. Gruber C, Gruber D. Bazedoxifene (Wyeth). *Curr Opin Invest Drugs*. 2004;5:1086–1093.
5. Miller CP, Harris HA, Komm BS. Bazedoxifene acetate: selective estrogen receptor modulator treatment and prevention of osteoporosis. *Drugs Future*. 2002;27:117–121.
6. Komm BS, Kharode YP, Bodine PV, Harris HA, Miller CP, Lyttle CR. Bazedoxifene acetate: a selective estrogen receptor modulator with improved selectivity. *Endocrinology*. 2005;146:3999–4008.
7. Lewis-Wambi JS, Kim H, Curpan R, Grigg R, Sarker MA, Jordan VC. The selective estrogen receptor modulator bazedoxifene inhibits hormone-independent breast cancer cell growth and down-regulates estrogen receptor α and cyclin D1. *Mol Pharmacol*. 2011;80:610–620.
8. Jeselsohn R. *A study of palbociclib in combination with bazedoxifene in hormone receptor positive breast cancer*. Dana-Farber Cancer Institute; 2017. ClinicalTrials.gov.
9. Lindsay R, Gallagher JC, Kagan R, Pickar JH, Constantine G. Efficacy of tissue-selective estrogen complex of bazedoxifene/conjugated estrogens for osteoporosis prevention in at-risk postmenopausal women. *Fertil Steril*. 2009;92:1045–1052.
10. Meunier B. Hybrid molecules with a dual mode of action: dream or reality? *Acc Chem Res*. 2008;41:69–77.
11. Mayur YC, Peters GJ, Rajendra Prasad VVS, Lemos C, Sathish NK. Design of new drug molecules to be used in reversing multidrug resistance in cancer cells. *Curr Cancer Drug Targets*. 2009;9:298–306.
12. Solomon VR, Hu C, Lee H. Hybrid pharmacophore design and synthesis of isatin-benzothiazole analogs for their anti-breast cancer activity. *Bioorg Med Chem*. 2009;17:7585–7592.
13. Al-Omran F, Mohareb RM, El-Khair AA. New route for synthesis, spectroscopy, and X-ray studies of 2-[aryl-(6′-hydroxy-4′, 4′-dimethyl-2′-oxocyclohex-6′-enyl) methyl]-3-hydroxy-5, 5-dimethylcyclohex-2-enone and 1, 8-dioxo-octahydroxanthenes and antitumor evaluation. *Med Chem Res*. 2014;23:1623–1633.
14. Giannouli V, Kostakis IK, Pouli N, et al. Design, synthesis, and evaluation of the antiproliferative activity of a series of novel fused xanthenone aminoderivatives in human breast cancer cells. *J Med Chem*. 2007;50:1716–1719.
15. Rachner TD, Schoppet M, Niebergall U, Hofbauer LC. 17β-Estradiol inhibits osteoprotegerin production by the estrogen receptor-α-positive human breast cancer cell line MCF-7. *Biochem Biophys Res Comm*. 2008;368:736–741.
16. Siqueira de Oliveira AP, Ferreira de Sousa J, Aparecido da Silva M, et al. Estrogenic and chemopreventive activities of xanthones and flavones of Syngonanthus (Eriocaulaceae). *Steroids*. 2013;78:1053–1063.
17. Shin Y, Han S, De U, et al. Ru(II)-catalyzed selective C-H amination of xanthones and chromones with sulfonyl azides: synthesis and anticancer evaluation. *J Org Chem*. 2014;79:9262–9271.
18. Kozlov NG, Gusak KN. 3-(4-Fluorophenyl)-1H-pyrazole-4-carbaldehyde in the synthesis of aza- and diazaphenanthrene derivatives. *Russ J Org Chem*. 2007;43:241–248.
19. Ferreira MS, Pires DAT, Figueroa-Villar JD. Evaluation of tetraketones and xanthenediones as tyrosinase inhibitors or activators. *World J Pharm Pharma Sci*. 2015;4:1705–1718.
20. Kuete V, Sandjo LP, Ouete JLN, Fouotsa H, Wiench B, Efferth T. Cytotoxicity and modes of action of three naturally occurring xanthones (8-hydroxycudraxanthone G, morusignin I and cudraxanthone I) against sensitive and multidrug-resistant cancer cell lines. *Phytomed*. 2014;21:315–322.
21. Hartati S, Triyono IK, Handayani S. Cytotoxic isobractatin (prenylated xanthone) epimer mixture of Garcinia eugenifolia. *Indones J Chem*. 2014;14:277–282.
22. da Silva DL, Terra BS, Lage MR, et al. Xanthenones: calixarenes-catalyzed syntheses, anticancer activity and QSAR studies. *Org Biomol Chem*. 2015;13:3280–3287.
23. Kumar A, Sharma S, Maurya RA, Sarkar J. Diversity oriented synthesis of benzoxanthene and benzochromene libraries via one-pot, three-component reactions and their anti-proliferative activity. *J Comb Chem*. 2009;12:20–24.
24. Wang TTY, Milner MJ, Milner JA, Kim YS. Estrogen receptor α as a target for indole-3-carbinol. *J Nutr Biochem*. 2006;17:659–664.
25. Kim YS, Milner J. Targets for indole-3-carbinol in cancer prevention. *J Nutr Biochem*. 2005;16:65–73.
26. Sidhu JS, Singla R, Mayank, Jaitak V. Indole derivatives as anticancer agents for breast cancer therapy: a review. *Anti-Cancer Agents Med Chem*. 2015;16:160–173.
27. Greenberger LM, Annable T, Collins KI, et al. A new antiestrogen, 2-(4-hydroxy-phenyl)-3-methyl-1-[4-(2-piperidin-1-yl-ethoxy)-benzyl]-1H-indol-5-ol hydrochloride (ERA-923), inhibits the growth of tamoxifen-sensitive and-resistant tumors and is devoid of uterotropic effects in mice and rats. *Clin Cancer Res*. 2001;10:3166–3177.
28. Singh V, Fedeles BI, Essigmann JM. Role of tautomerism in RNA biochemistry. *RNA*. 2015;21:1–13.
29. Geohagen BC, Vydyanathan A, Kosharskyy B, Shaparin N, Gavin T, LoPachin RM. Enolate-forming phloretin pharmacophores: hepatoprotection in an experimental model of drug-induced toxicity. *J Pharmacol Exp Ther*. 2016;357:476–486.
30. Mandic Z, Gabelica V. Ionization, lipophilicity and solubility properties of repaglinide. *J Pharm Biomed Anal*. 2006;41:866–871.
31. Al-Bader M, Ford C, Al-Ayadhy B, Francis I. Analysis of estrogen receptor isoforms and variants in breast cancer cell lines. *Exp Ther Med*. 2011;2:537–544.
32. Strom A, Hartman J, Foster JS, Kietz S, Wimalasena J, Gustafsson JA. Estrogen receptor beta inhibits 17beta-estradiol-stimulated proliferation of the breast cancer cell line T47D. *Proc Natl Acad Sci USA*. 2004;101:1566–1571.
33. Fang YQ, Weng YZ, Huang WQ, Sun L. Localization of the estrogen receptor alpha and beta-subtype in the nervous system, Hatschek's pit and gonads of amphioxus, Branchiostoma belcheri. *Shi Yan Sheng Wu Xue Bao*. 2003;36:368–374.
34. Kurebayashi J, Otsuki T, Kunisue H, Tanaka K, Yamamoto S, Sonoo H. Expression levels of estrogen receptor-α, estrogen receptor-β, coactivators, and corepressors in breast cancer. *Clin Cancer Res*. 2000;6:512–518.
35. Osborne CK, Schiff R. Mechanisms of endocrine resistance in breast cancer. *Ann Rev Med*. 2011;62:233–247.
36. Dhiman M, Zago MP, Nunez S, et al. Cardiac-oxidized antigens are targets of immune recognition by antibodies and potential molecular determinants in chagas disease pathogenesis. *PLoS One*. 2012;7:e28449.
37. Mantha AK, Dhiman M, Taglialatela G, Perez-Polo RJ, Mitra S. Proteomic study of amyloid beta (25–35) peptide exposure to neuronal cells: impact on APE1/Ref-1's protein–protein interaction. *J Neuro Res*. 2012;90:1230–1239.
38. Kruger NJ. The Bradford method for protein quantitation. In: Walker JM, ed. *The Protein Protocols Handbook*. Totowa, NJ: Humana Press; 2009:17–24.